Available online at www.sciencedirect.com
ScienceDirect
Scripta Materialia 59 (2008) 1210–1213
Scripta MATERIALIA
www.elsevier.com/locate/scriptamat

Stress-induced softening and hardening in a bulk metallic glass

L.Y. Chen,[a] Q. Ge,[b] S. Qu[b,*] and J.Z. Jiang[a,*]

[a] *International Center for New-Structured Materials (ICNSM), Zhejiang University and Laboratory of New-Structured Materials, Department of Materials Science and Engineering, Zhejiang University, Hangzhou 310027, PR China*
[b] *International Center for New-Structured Materials (ICNSM), Zhejiang University and Institute of Applied Mechanics, School of Aeronautics and Astronautics, Zhejiang University, Hangzhou 310027, PR China*

Received 20 June 2008; revised 4 August 2008; accepted 13 August 2008
Available online 2 September 2008

To uncover the influence of pre-existing/residual stress on the mechanical behavior of metallic glass, the micro-Vickers indentation of a stressed metallic glass was studied. The pre-existing stress was introduced by bending. The results show that the nominal hardness decreases with pre-existing tensile stress and increases with pre-existing compressive stress. The real hardness decreases with pre-existing tensile stress, but does not increase obviously with pre-existing compressive stress. The mechanism of the strong hardness dependence on stress was investigated using finite element analysis. The unexpected hardness dependence on pre-existing compressive stress is also discussed.

Keywords: Metallic glasses; Hardness; Shear bands; Residual stresses

Bulk metallic glasses (BMGs) exhibit the unique combination of high yield strength, high hardness, large elastic limit [1–3] and high strength reliability (high Weibull modulus) [4,5], which is of significant interest for applications. However, the poor plasticity and low fatigue resistance seriously restrict their applicability [3,6,7]. A number of efforts, including introducing chemical/structural heterogeneity [8–17], searching for alloys with high Poisson's ratios [18,19] or tailoring the amount of free volume [20,21], have been made to improve the plasticity as well as the fatigue resistance of BMGs. Recently, the enhancement of plasticity by shot-peening-induced residual stress [22], and loading-induced stress gradients [23] were reported. The influence of residual stress on fatigue resistance has also been investigated [24,25]. These reports reveal that tailoring the stress in BMGs is a practical and promising way to improve their mechanical performance. Thus, understanding the influence of pre-existing stress on the mechanical response of BMGs is essential. The purpose of this work is to address this issue, focusing on the influence of pre-existing stress on hardness, by micro-Vickers indentation. The evolution of hardness, indented impression and shear band distribution around the indenter with stress is demonstrated and discussed.

$Cu_{45}Zr_{46.5}Al_7Ti_{1.5}$ alloy ingots were prepared by arc melting the mixtures of Cu (99.9 wt.%), Zr (99.8 wt.%), Al (99.9 wt.%) and Ti (99.9 wt.%) elements in Ti-gettered high-purity argon atmosphere. Rectangular alloy bars with a cross-section of 3×3 mm were prepared by injecting alloy melt into copper mold. Structures of samples were examined by X-ray diffractometry (XRD, Cu K_α radiation), high-resolution XRD (HRXRD, 100 keV, at HASYLAB, Germany) and transmission electron microscopy (TEM, Hitachi H-9000NAR). Glass transition and crystallization behavior were studied by differential scanning calorimetry (DSC) using a Netzsch DSC 404 C under a continuous argon flow at a heating rate of 0.33 K s^{-1}. The pre-existing stress was applied by bending using a home-made apparatus presented below. Indentation experiments were conducted with a micro-Vickers hardness tester (MH-5, Everone, China). Morphology and shear band distribution of the indented impression were observed by field emission scanning electron microscopy (FESEM, Hitachi S-4800).

Figure 1a shows the facility for introducing pre-existing stress by bending as well as the bent specimen fixed in the apparatus. The specimen for bending tests with a size of $2.2 \times 2.2 \times 35$ mm was cut, milled and polished

* Corresponding authors. Tel.: +86 87952107 (J.Z. Jiang); e-mail addresses: squ@zju.edu.cn; jiangjz@zju.edu.cn

1359-6462/$ - see front matter © 2008 Acta Materialia Inc. Published by Elsevier Ltd. All rights reserved.
doi:10.1016/j.scriptamat.2008.08.021

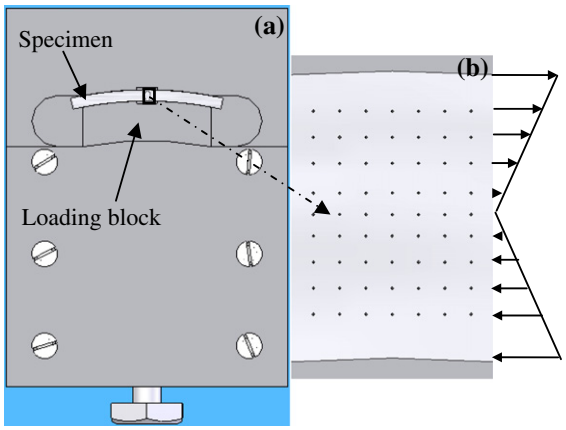

Figure 1. (a) Schematic diagrams of the artificially bent specimen fixed in the apparatus and (b) the enlargement of the squared part in (a), which shows the distribution of the indentations made on middle part of the specimen. The stress on the cross-section of the specimen induced by bending is also shown.

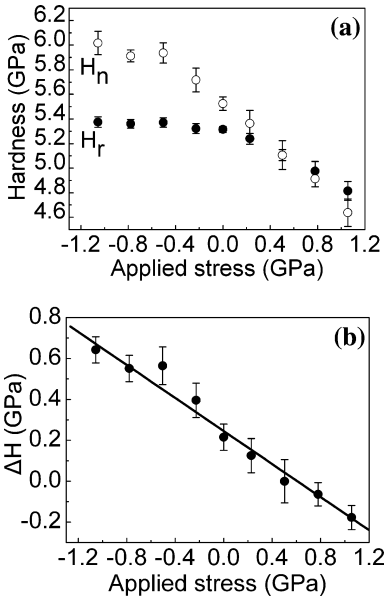

Figure 2. (a) The stress dependence of the nominal hardness H_n (calculated from the diagonal length of the impression without concerning the pile-up and sink-in effects) and the real hardness H_r (calculated from the real projected contact area). (b) The stress dependence of ΔH (the difference between nominal hardness H_n and real hardness H_r).

from the as-cast alloy bar with a cross-section of 3×3 mm. Before bending, the amorphous nature of the specimen was verified by HRXRD, TEM and DSC, and the homogeneity of the hardness around the specimen was also checked. When bent elastically, the applied stress on the surface of the bar varied linearly from the largest tension at the top to the largest compression at the bottom as shown in Figure 1b. Several linear arrays of indentations were made on the surface of the bar by micro-Vickers hardness tester, allowing for the acquisition of the hardness data at numerous tensile and compressive uniaxial stresses, as shown in Figure 1b. The magnitude and the sign of the stress at each indentation were calculated from the strain that the position of the indentation undertakes under bending. The load and the dwell time used for micro-Vickers hardness test are 2 N and 15 s, respectively.

The Meyer hardness at nine different stress levels was obtained according to a standard method (measuring the diagonal length of the impression) during micro-Vickers indentation experiments. The hardness value obtained by this way was assigned as nominal hardness (H_n) hereafter. Figure 2a demonstrates the stress dependence of the nominal hardness H_n. H_n decreases from 5.5 to 4.6 GPa (i.e. ~16% reduction) under 1.05 GPa tensile stress and increases from 5.5 to 6.0 GPa (i.e. ~9% increase) under 1.05 GPa compressive stress. The maximum change of nominal hardness in the present BMG is about 25%, which is much larger than the maximum value about 10% reported for crystalline alloys [26]. It should be stressed that the recent research indicates that the stress dependence of nominal hardness in a crystalline alloy is the result of the mis-estimation of the projected contact area [26,27]. When the hardness data were deduced by measuring the diagonal length of the impression in the micro-Vickers hardness test or from the load–displacement curve in the instrumented indentation experiment, the pile-up and sink-in induced by applied stress were not fully considered, which results in the mis-evaluation of the projected area [26,27]. If the real projected contact area was used to deduce the hardness data, no stress dependence of hardness was detected in the crystalline alloy [26,27]. To check whether the applied stress can induce a change in the real hardness (calculated from the real projected contact area, referred to hereafter as H_r), the intended impressions on the $Cu_{45}Zr_{46.5}Al_7Ti_{1.5}$ BMG in this work were all imaged by SEM. Three representative impressions, at 1.05 GPa tensile stress, zero stress and 1.05 GPa compressive stress, are shown in Figure 3. It is clear that the edges of the impressions are curved inward in Figure 3a due to sink-in, but curved outward in Figure 3c due to pile-up. The real projected areas were measured through outlining the contact perimeter and determining the number of pixels in the enclosed region. Then, the real hardness was calculated based on the real projected contact area. Contrary to the case for the crystalline alloy [26,27], the applied stress indeed induces a change in the hardness in this BMG, as shown in Figure 2a. It is found that the change is asymmetric: the real hardness decreases with applied tensile stress, but the increase in real hardness with compressive stress cannot be detected. Figure 2b illustrates the difference (ΔH) between nominal hardness H_n and real hardness H_r. It is found that ΔH changes linearly with applied stress with a slope of 0.4 and arises from the pile-up or sink-in. Thus, the linearity of ΔH vs. stress indicates that the stress-induced pile-up or sink-in changes linearly with applied stress. This result could be useful for characterizing pre-existing/residual stress in BMGs.

A simple explanation to the real hardness dependence on applied stress is given by yield locus, as shown in Figure 4. It is apparent that the indentation stress required for yielding increases as the applied stress changes from 1.05 to –1.05 GPa (marked by arrow). Consequently, an increase in real hardness is expected. Since this analysis is based entirely on the initial stress state in the speci-

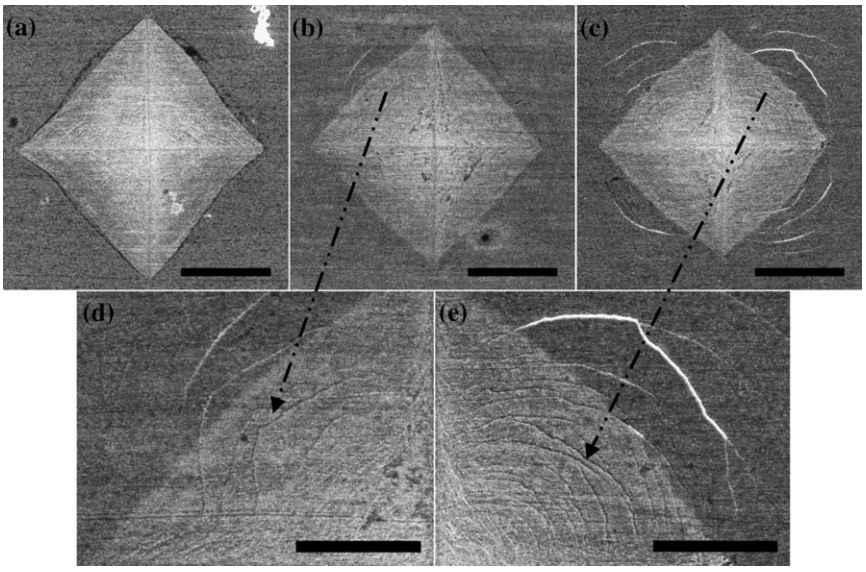

Figure 3. SEM images of the indentations made at uniaxial stress of (a) 1.05 GPa (tension), (b) 0 GPa (without stress) and (c) –1.05 GPa (compression); (d) and (e) are enlargements of (b) and (c), respectively. The lengths of scale bars are 10 μm in (a), (b) and (c), 5 μm in (d) and (e).

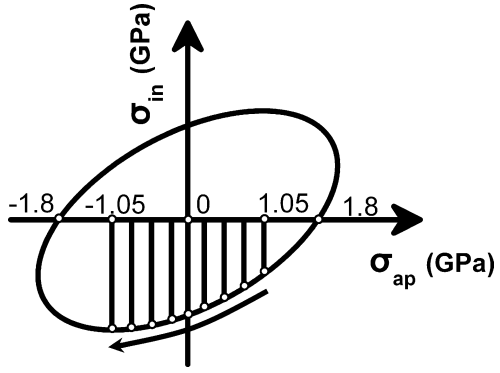

Figure 4. Yield locus for von Mises criterion drawn based on the compressive yield strength of $Cu_{45}Zr_{46.5}Al_7Ti_{1.5}$ BMG. σ_{ap} and σ_{in} denote the applied stress and indentation stress, respectively.

men, the influence of the localized plastic deformation on the stress state in the vicinity of the indenter is not considered. To further understand the stress dependence of H_r in BMGs, finite element analysis was conducted using the commercial software ABAQUS. To simplify the analysis, the Vickers pyramid indenter used in the experiment was approximated by a rigid cone with a half-included tip angle of 70.3°, which gives the same depth-to-area ratio as the Vickers pyramid. The specimen was represented by a bar with the same yield strength, 1.8 GPa, elastic modulus, 92 GPa, and Poisson's ratio, 0.368, for the $Cu_{45}Zr_{46.5}Al_7Ti_{1.5}$ metallic glassy bar used for indentation measurements. The pre-existing stress was applied by bending as in the experiment. The elastic–perfectly plastic constitutive behavior with von Mises yield criterion was used for simulation. Figure 5a shows the simulated results at the tension side together with the experimental data. The simulated data captures the trend of the hardness dependence on stress well. The most likely reasons for the slight difference in the results between the simulation and the experiment are (i) different shapes of indenters

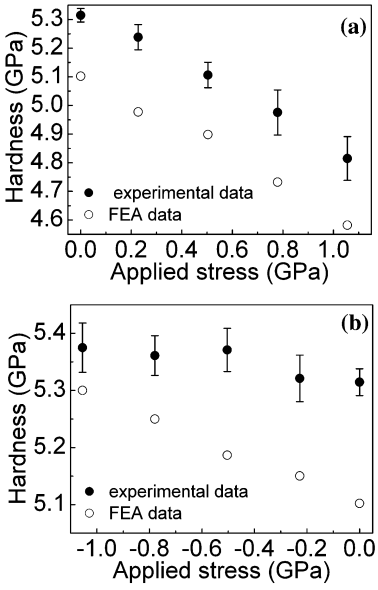

Figure 5. Hardness deduced from finite element analysis of (a) the tension side and (b) the compression side. The hardness data obtained by experiment are also shown for comparison.

used (i.e. Vickers indenter in experiment while conical one in simulation) and (ii) the fact that the von Mises yield criterion used in simulation underestimated the hardness of the BMG [28–30]. In addition, we also performed a few simulations with the same yield locus for various ratios of yield strength to elastic modulus. It is found that the stress dependence of hardness decreases as the ratio of yield strength to elastic modulus decreases. This indicates that the unique combination of the high yield strength and low elastic modulus or large elastic limit for BMGs is the reason for the stress dependence of hardness for the BMG, which is consistent with the results in Ref. [31]. However, the simulation results for the compression side cannot capture the trend well:

the slope of the experimental results is lower than that of the simulated ones. To address this issue, we carefully examined the shear band distribution on the impression. It is found that the pre-existing compressive stress induced formation of high-density shear bands as shown in Figure 3e, which may result in softening [32,33], while a low number of shear bands were detected on the surface at zero stress (Fig. 3d). It is not unreasonable to expect that the lower enhancement of hardness obtained from experiments is due to a softening effect induced by the high-density of shear bands. For the relationship of density of shear bands with compressive stress, we suggest that the shear displacement of a shear banding event is dependent on the normal stress on the shear plane. The higher the normal stress, the smaller the shear displacement. An increase in the applied compressive stress results in an increase of the normal stress on the shear plane. Thus, a smaller shear displacement is expected on the compression side. To accommodate the plastic deformation, formation of high-density shear bands is required.

In conclusion, the influence of the applied stress on indentation behavior of a $Cu_{45}Zr_{46.5}Al_7Ti_{1.5}$ BMG was investigated. The nominal hardness decreases with applied tensile stress and increases with applied compressive stress. The real hardness decreases with applied tensile stress, but does not increase with compressive stress obviously. Finite element analysis indicates that the strong hardness dependence on stress results from the large elastic limit of BMGs. Compressive stress induced the formation of high-density shear bands, which results in softening, reducing the enhancement of hardness induced by applied compressive stress. The results obtained in this work are helpful to understand the mechanical behavior of BMGs. The relationship of ΔH vs. applied stress reported here indicates that the indentation technique might be a promising method to characterize residual stress in BMGs.

The authors appreciate Mr. S.Q. Ding for his assistance in sample preparation, Dr. X.M. Huang and M.Y. Ge for their assistance in preparation of Figures 1 and 4 and Mr G.Q. Xie, M.F. Luo and Y.Z. Fang for SEM. The authors are grateful to Prof. K.Y. Zeng at the National University of Singapore for his valuable comments and suggestions. The authors acknowledge the anonymous referee for his/her profound suggestions. The authors thank HASYLAB in Germany, BSRF in Beijing, NSRL in Hefei, KEK in Japan, and APS in the USA for use of the synchrotron radiation facilities. Financial support from the National Natural Science Foundation of China (Grant Nos. 50425102, 50601021, 50701038, 60776014 and 10702062), Zhejiang University–Helmholtz cooperation fund, the Ministry of Education of China (Program for Changjiang Scholars and the Research Fund for the Doctoral Program of Higher Education), the Department of Science and Technology of Zhejiang province and Zhejiang University are gratefully acknowledged.

[1] W.L. Johnson, MRS Bull. 24 (1999) 42.
[2] A. Inoue, Acta Mater. 48 (2000) 279.
[3] C.A. Schuh, T.C. Hufnagel, U. Ramamurty, Acta Mater. 55 (2007) 4067.
[4] W.F. Wu, Y. Li, C.A. Schuh, Philos. Mag. 88 (2008) 71.
[5] J.H. Yao, J.Q. Wang, L. Lu, Y. Li, Appl. Phys. Lett. 92 (2008) 041905.
[6] B.C. Menzel, R.H. Dauskardt, Scr. Mater. 55 (2006) 601.
[7] C.E. Packard, L.M. Witmer, C.A. Schuh, Appl. Phys. Lett. 92 (2008) 171911.
[8] C.C. Hays, C.P. Kim, W.L. Johnson, Phys. Rev. Lett. 84 (2000) 2901.
[9] C. Fan, R.T. Ott, T.C. Hufnagel, Appl. Phys. Lett. 81 (2002) 1020.
[10] M.L. Lee, Y. Li, C.A. Schuh, Acta Mater. 52 (2004) 4121.
[11] T. Wada, A. Inoue, A.L. Greer, Appl. Phys. Lett. 86 (2005) 251907.
[12] Y.C. Kim, J.H. Na, J.M. Park, D.H. Kim, J.K. Lee, W.T. Kim, Appl. Phys. Lett. 83 (2003) 3093.
[13] J. Das, M.B. Tang, K.B. Kim, R. Theissmann, F. Baier, W.H. Wang, J. Eckert, Phys. Rev. Lett. 94 (2005) 205501.
[14] J. Saida, A.D.H. Setyawan, H. Kato, A. Inoue, Appl. Phys. Lett. 87 (2005) 151907.
[15] S.W. Lee, M.Y. Huh, E. Fleury, J.C. Lee, Acta Mater. 54 (2006) 349.
[16] M.W. Chen, A. Inoue, W. Zhang, T. Sakurai, Phys. Rev. Lett. 96 (2006) 245502.
[17] D.C. Hofmann, J.Y. Suh, A. Wiest, G. Duan, M.L. Lind, M.D. Demetriou, W.L. Johnson, Nature 451 (2008) 1085.
[18] J. Schroers, W.L. Johnson, Phys. Rev. Lett. 93 (2004) 255506.
[19] Y.H. Liu, G. Wang, R.J. Wang, D.Q. Zhao, M.X. Pan, W.H. Wang, Science 315 (2007) 1385.
[20] L.Y. Chen, Z.D. Fu, G.Q. Zhang, X.P. Hao, Q.K. Jiang, X.D. Wang, Q.P. Cao, H. Franz, Y.G. Liu, H.S. Xie, S.L. Zhang, B.Y. Wang, Y.W. Zeng, J.Z. Jiang, Phys. Rev. Lett. 100 (2008) 075501.
[21] L.Y. Chen, A.D. Setyawan, H. Kato, A. Inoue, G.Q. Zhang, J. Saida, X.D. Wang, J.Z. Jiang, Scr. Mater. 59 (2008) 75.
[22] Y. Zhang, W.H. Wang, A.L. Greer, Nat. Mater. 5 (2006) 857.
[23] L.Y. Chen, Q. Ge, S. Qu, Q.K. Jiang, X.P. Nie, J.Z. Jiang, Appl. Phys. Lett. 92 (2008) 211905.
[24] M.E. Launey, R. Busch, J.J. Kruzic, Acta Mater. 56 (2008) 500.
[25] R. Raghavan, R. Ayer, H.W. Jin, C.N. Marzinsky, U. Ramamurty, Scr. Mater. 59 (2008) 167.
[26] T.Y. Tsui, W.C. Oliver, G.M. Pharr, J. Mater. Res. 11 (1996) 752.
[27] A. Bolshakov, W.C. Oliver, G.M. Pharr, J. Mater. Res. 11 (1996) 760.
[28] R. Vaidyanathan, M. Dao, G. Ravichandran, S. Suresh, Acta Metall. 49 (2001) 3781.
[29] C.A. Schuh, A.C. Lund, Nat. Mater. 2 (2003) 449.
[30] M.N.M. Patnaik, R. Narasimhan, U. Ramamurty, Acta Mater. 52 (2004) 3335.
[31] X. Chen, J. Yan, A.M. Karlsson, Mater. Sci. Eng. A 416 (2007) 139.
[32] H. Bei, S. Xie, E.P. George, Phys. Rev. Lett. 96 (2006) 105503.
[33] R. Bhowmick, R. Raghavan, K. Chattopadhyay U. Ramamurty, Acta Mater. 54 (2006) 4221.